Important Notice to Authors

No further publication processing will occur until we receive your response to this proof.

Attached is a PDF proof of your forthcoming article in *Physical Review Letters*. The article accession code is LY15956. Your paper will be in the following section of the journal: LETTERS — Elementary Particles and Fields

Please note that as part of the production process, APS converts all articles, regardless of their original source, into standardized XML that in turn is used to create the PDF and online versions of the article as well as to populate third-party systems such as Portico, Crossref, and Web of Science. We share our authors' high expectations for the fidelity of the conversion into XML and for the accuracy and appearance of the final, formatted PDF. This process works exceptionally well for the vast majority of articles; however, please check carefully all key elements of your PDF proof, particularly any equations or tables.

Figures submitted electronically as separate files containing color appear in color in the online journal. However, all figures will appear as grayscale images in the print journal unless the color figure charges have been paid in advance, in accordance with our policy for color in print (https://journals.aps.org/authors/color-figures-print).

Specific Questions and Comments to Address for This Paper

The numbered items below correspond to numbers in the margin of the proof pages pinpointing the source of the question and/or comment. The numbers will be removed from the margins prior to publication.

Q: Please check that all references include complete titles.

- I Second proof: Please carefully confirm that all first-proof corrections were addressed and that changes were made accurately.
- 2 Second proof: Please check and approve that the paper is ready to be published in its current form.

Titles in References

The editors now encourage insertion of article titles in references to journal articles and e-prints. This format is optional, but if chosen, authors should provide titles for *all* eligible references. If article titles remain missing from eligible references, the production team will remove the existing titles at final proof stage.

Funding Information

Information about an article's funding sources is now submitted to Crossref to help you comply with current or future funding agency mandates. Crossref's Open Funder Registry (https://www.crossref.org/services/funder-registry/) is the definitive registry of funding agencies. Please ensure that your acknowledgments include all sources of funding for your article following any requirements of your funding sources. Where possible, please include grant and award ids. Please carefully check the following funder information we have already extracted from your article and ensure its accuracy and completeness:

- National Science Foundation, FundRef ID http://dx.doi.org/10.13039/100000001 (US/United States)
- MEPhI Academic Excellence Project
- Russian Foundation for Basic Research, FundRef ID http://dx.doi.org/10.13039/501100002261 (RU/Russian Federation)
- U.S. Department of Energy, FundRef ID http://dx.doi.org/10.13039/100000015 (US/United States)

Other Items to Check

- Please note that the original manuscript has been converted to XML prior to the creation of the PDF proof, as described above. Please carefully check all key elements of the paper, particularly the equations and tabular data.
- Title: Please check; be mindful that the title may have been changed during the peer-review process.
- Author list: Please make sure all authors are presented, in the appropriate order, and that all names are spelled correctly.
- Please make sure you have inserted a byline footnote containing the email address for the corresponding author, if desired. Please note that this is not inserted automatically by this journal.
- Affiliations: Please check to be sure the institution names are spelled correctly and attributed to the appropriate author(s).
- Receipt date: Please confirm accuracy.
- Acknowledgments: Please be sure to appropriately acknowledge all funding sources.
- References: Please check to ensure that titles are given as appropriate.
- Hyphenation: Please note hyphens may have been inserted in word pairs that function as adjectives when they occur before a noun, as in "x-ray diffraction," "4-mm-long gas cell," and "R-matrix theory." However, hyphens are deleted from word pairs when they are not used as adjectives before nouns, as in "emission by x rays," "was 4 mm in length," and "the R matrix is tested."

 Note also that Physical Review follows U.S. English guidelines in that hyphens are not used after prefixes or before suffixes: superresolution, quasiequilibrium, nanoprecipitates, resonancelike, clockwise.
- Please check that your figures are accurate and sized properly. Make sure all labeling is sufficiently legible. Figure quality in this proof is representative of the quality to be used in the online journal. To achieve manageable file size for online delivery, some compression and downsampling of figures may have occurred. Fine details may have become somewhat fuzzy, especially in color figures. The print journal uses files of higher resolution and therefore details may be sharper in print. Figures to be published in color online will appear in color on these proofs if viewed on a color monitor or printed on a color printer.
- Overall, please proofread the entire *formatted* article very carefully. The redlined PDF should be used as a guide to see changes that were made during copyediting. However, note that some changes to math and/or layout may not be indicated.

Ways to Respond

- Web: If you accessed this proof online, follow the instructions on the web page to submit corrections.
- Email: Send corrections to aps-robot@luminad.com. Include the accession code LY15956 in the subject line.
- Fax: Return this proof with corrections to +1.855.808.3897.

If You Need to Call Us

You may leave a voicemail message at +1.855.808.3897. Please reference the accession code and the first author of your article in your voicemail message. We will respond to you via email.

3

4

5 6

7

8

9 10

11

12 13

14

15

16

17

19 20

21

22

23

24

25

26

27

28

29

30

31

32

33

34

35

36

37

38

39

40

41

42

43

18 1

Kink-Kink and Kink-Antikink Interactions with Long-Range Tails

Ivan C. Christov, Robert J. Decker, A. Demirkaya, Vakhid A. Gani, P. G. Kevrekidis, Avinash Khare,⁶ and Avadh Saxena⁷ ¹School of Mechanical Engineering, Purdue University, West Lafayette, Indiana 47907, USA ²Mathematics Department, University of Hartford, West Hartford, Connecticut 06117, USA ³Department of Mathematics, National Research Nuclear University MEPhI (Moscow Engineering Physics Institute), 115409 Moscow, Russia ⁴Theory Department, National Research Center Kurchatov Institute, Institute for Theoretical and Experimental Physics, 117218 Moscow, Russia ⁵Department of Mathematics and Statistics, University of Massachusetts, Amherst, Massachusetts 01003, USA ⁶Physics Department, Savitribai Phule Pune University, Pune 411007, India ⁷Theoretical Division and Center for Nonlinear Studies, Los Alamos National Laboratory,

Los Alamos, New Mexico 87545, USA

(Received 21 November 2018; revised manuscript received 5 March 2019)

In this Letter, we address the long-range interaction between kinks and antikinks, as well as kinks and kinks, in φ^{2n+4} field theories for n>1. The kink-antikink interaction is generically attractive, while the kink-kink interaction is generically repulsive. We find that the force of interaction decays with the 2n/(n-1)th power of their separation, and we identify the general prefactor for arbitrary n. Importantly, we test the resulting mathematical prediction with detailed numerical simulations of the dynamic field equation, and obtain good agreement between theory and numerics for the cases of n=2 (φ^8 model), n=3 (ω^{10} model), and n=4 (ω^{12} model).

DOI:

Introduction.—The study of field-theoretic models with polynomial potentials has been a topic of wide appeal across a diverse span of theoretical physics areas, including notably cosmology, condensed matter physics, and nonlinear dynamics [1-3]. Arguably, the most intensely studied model in this class is the quartic (double well) potential, the so-called φ^4 model, connected to the phenomenological Ginzburg-Landau theory [4,5], among numerous other applications [6–9]. While the φ^4 model has a time-honored history in its own right [10], more recently, higher-order field theories have emerged as models of phase transitions [11] relevant to materials science [12-14] (see also Ref. [10] (Chap. 11) and Ref. [15]), or in quantum mechanical problems (including supersymmetric ones) [16], among others. There, the prototypical example has been the φ^6 field-theoretic model, which has led to numerous insights and novel possibilities with respect to the spectral properties [17] and wave interactions [18].

Scattering of solitary waves (topological defects or otherwise) is a long-standing topic of active research

Published by the American Physical Society under the terms of the Creative Commons Attribution 4.0 International license. Further distribution of this work must maintain attribution to the author(s) and the published article's title, journal citation, and DOI. Funded by SCOAP³.

[19], starting from the early works [7,8]. Our aim here is to go beyond the "classical" models, in a direction that, admittedly, has already seen some significant activity [11,20–26]. One of the particularly appealing aspects of this research program (aside from its potential abovementioned applications in materials science or high-energy physics or quantum mechanics) is that higher-order field theories possess topological defect solutions (kinks) with power-law tails, rather than the "standard" exponential tails that we are used to in the φ^4 and the (usual variants of) φ^6 field theories. The resulting dynamics set by the power-law tails endows topological defects with long-range interactions. Recently, a methodology for quantifying such kink-kink and kink-antikink interactions in the ω^8 model was proposed in Ref. [27]. In our previous work [28], we showed that there are some deep challenges in even initializing such topological defect configurations numerically. Thus, the initial conditions in a direct numerical simulation of interactions may substantially affect the nature of the observed interactions (cf. also earlier works including, e.g., Ref. [26]).

45

46

47

48

49

50

51

52

53

54

55

56

57

58

59

60

61

62

63

64

65

66

67

69

One of the related motivations of our study stems from the expectation that power-law tails may affect the physical properties of a system governed by higher-order field theories. For instance, the dynamics and interaction of domain walls in ferroelastic materials undergoing successive phase transitions [13] should affect the elastic properties in unusual ways. Similarly, the response of crystals undergoing isostructural transitions [14] or the behavior of crystallization of chiral proteins [29] should be altered by the associated long-range interactions between domain walls.

The present effort provides an answer to the question of how kink-kink (K-K) and kink-antikink (K-AK) long-range (power-law) interactions occur in higher-order field theories that exhibit such topological defects. We consider particular (yet highly relevant to this problem) potentials for which the highest power of φ in the potential is 2n + 4, and we analyze the interaction for arbitrary $n \ge 2$. We find that kinks repel each other, while kinks and antikinks generically attract, in both cases with a power law decaying as the (2n/n-1)th power of their mutual separation. Furthermore, we adapt the recent methodology of Ref. [27] to the case of arbitrary $n \ge 2$, and we identify the prefactor (distinct for K-K and K-AK) of the corresponding power-law interaction force. Equally important, we resolve the "uncertainty" of the prefactor indicated in Ref. [27]. We identify the most accurate asymptotic prefactor and test it against direct numerical simulations to find good agreement for φ^8 (n=2), φ^{10} (n=3), and φ^{12} (n = 4) models, for both K-K and K-AK interactions. The increasing trend of the deviations between the two, as nincreases, is also explained.

First, we present our theoretical results. Then, we compare them to direct numerical simulations. Finally, we offer some conclusions and directions for future work.

Theoretical analysis.—Consider a real scalar field $\varphi(x,t)$ in (1+1) dimensional spacetime, its dynamics set by the Lagrangian density

$$\mathcal{L} = \frac{1}{2} \left(\frac{\partial \varphi}{\partial t} \right)^2 - \frac{1}{2} \left(\frac{\partial \varphi}{\partial x} \right)^2 - V(\varphi). \tag{1}$$

103 The dynamic equation of motion of this field is

$$\frac{\partial^2 \varphi}{\partial t^2} = \frac{\partial^2 \varphi}{\partial x^2} - \frac{dV}{d\varphi}.$$
 (2)

The potential V is, specifically, of the form

$$V(\varphi) = \frac{1}{2}(1 - \varphi^2)^2 \varphi^{2n}.$$
 (3)

This potential has three minima: $\bar{\varphi}_1 = -1$, $\bar{\varphi}_2 = 0$, and $\bar{\varphi}_3 = 1$. Hence, there are two kinks in this model, $\varphi_{(-1,0)}(x)$ and $\varphi_{(0,1)}(x)$, and two corresponding antikinks, $\varphi_{(0,-1)}(x)$ and $\varphi_{(1,0)}(x)$. All of these defects exhibit one power-law and one exponential asymptotic decay to the respective equilibria (0 and ± 1) as $|x| \to \infty$. We study the interaction force between the kink $\varphi_{(0,1)}(x)$ and the kink $\varphi_{(-1,0)}(x)$. Their time-dependent positions are $x = \pm A(t)$, respec-tively, and their long-range tails overlap. Similarly, for

the K-AK interaction, we employ the antikink $\varphi_{(0,-1)}(x)$ and the corresponding mirror kink $\varphi_{(-1,0)}(x)$ located at $x = \pm A(t)$, respectively.

In Ref. [28], the interaction via power-law tail asymptotics was studied numerically for n=2 (φ^8 model). In Ref. [27], the force between a well-separated kink-kink and kink-antikink was analyzed, again for n=2. Our aim here is to generalize the (most sophisticated among the different) approach(es) of the very recent work [27], and to calculate the result for arbitrary n. Then, we blend this theoretical analysis with the delicate computational approach from Ref. [28] to fully flesh out the K-K and K-AK long-range interactions in such higher-order field theoretic models involving power-law tails.

Below, we model the accelerating kink solution of Eq. (2) by a field of the form $\varphi(x,t) = \phi(y)$, where y = x - A(t) and $\phi = \varphi_{(0,1)}$ or $\varphi_{(0,-1)}$.

Kink-kink interaction.—Substituting the kink profile into Eq. (2) yields the static equation for ϕ :

$$\phi'' + a\phi' - \frac{dV}{d\varphi}\Big|_{\varphi = \phi} = 0, \tag{4}$$

where $a = \ddot{A}$ is the acceleration (assumed small) and Lorentz contraction terms $(\propto \dot{A}^2)$ have been neglected. Here, $\dot{A} = dA/dt$, and $\phi' = d\phi/dy$. Following Ref. [27], the Bogomolny equation $\phi' = (dW/d\varphi)|_{\varphi=\phi}$, where $V = (1/2)(dW/d\varphi)^2$, is used to eliminate ϕ' from Eq. (4). Treating a as slowly varying, we define an effective potential $\tilde{V}(\phi) \approx V(\phi) - aW(\phi)$. Then, from the first integral of Eq. (4) (setting the constant of integration in the limit of $y \to \infty$), we obtain

$$\left(\frac{d\phi}{dy}\right)^2 = 2\tilde{V}(\phi) + 2aW(1) \sim \phi^{2n} + \frac{4a}{(n+1)(n+3)}.$$
 (5)

This calculation is asymptotic [dropping $o(\phi^{2n})$ terms], using the fact that our chosen family of potentials is such that $V(\phi) \sim \frac{1}{2}\phi^{2n}$ as $\phi \to 0$. Meanwhile, the second term in Eq. (5) (from the contribution of W(1) - W(0), independently of the normalization of W(1) is effectively proportional to the kink's rest mass M = 2/[(n+1)(n+3)] (for arbitrary n). Requesting (as in Ref. [27]) that $\phi(y)$ should have the properties that $\phi(-A) = 0$ while $\phi(0)$ diverges, we can rearrange Eq. (5) into a quadrature:

$$\int_0^\infty \frac{d\phi}{\sqrt{\phi^{2n} + \frac{4a}{(n+1)(n+3)}}} = A.$$
 (6)

The change of variables $\phi = (4a/[(n+1)(n+3)])^{1/2n}\lambda$ in 15% Eq. (6) yields

$$\left(\frac{4a}{(n+1)(n+3)}\right)^{(1-n)/2n} \int_0^\infty \frac{d\lambda}{\sqrt{\lambda^{2n}+1}} = A. \quad (7)$$

169 The relevant integral can be computed as

$$\int_0^\infty \frac{d\lambda}{\sqrt{\lambda^{2n} + 1}} = \frac{\Gamma(\frac{n-1}{2n})\Gamma(\frac{1}{2n})}{2n\sqrt{\pi}},\tag{8}$$

yielding the acceleration during the K-K interaction:

$$a = \left[\frac{\Gamma(\frac{n-1}{2n})\Gamma(\frac{1}{2n})}{2n\sqrt{\pi}} \right]^{2n/(n-1)} \frac{(n+1)(n+3)}{4} A^{2n/(1-n)}. \tag{9}$$

For the φ^8 model, n=2, and Eq. (9) yields $a=44.3139/A^4$. From Newton's second law (F=Ma), the force is $F=\frac{2}{15}a=5.9085/A^4$. Similarly, for the φ^{10} model, n=3, and we get $a=16.5411/A^3$ and $F=\frac{1}{12}a=1.3784/A^3$. Finally, for the φ^{12} model, n=4, and we get $a=16.1871/A^{8/3}$ and $F=\frac{2}{35}a=0.9250/A^{8/3}$.

Kink-antikink interaction.—The calculation in the K-AK case proceeds in the same way with the main difference that now $a = -\ddot{A}$ due to the attraction, in this case, between kink and antikink. From the corresponding version of Eq. (6), we have

$$\int_{\left[\frac{4a}{(n+1)(n+3)}\right]^{1/2n}}^{\infty} \frac{d\phi}{\sqrt{\phi^{2n} - \frac{4a}{(n+1)(n+3)}}} = A. \tag{10}$$

Notice that, now, the integral must be from the turning point rather than from 0, related to the sign change of the Bogomolny equation satisfied by the antikink.

Using the same change of variables as above, Eq. (10) becomes

$$\left[\frac{4a}{(n+1)(n+3)}\right]^{(1-n/2n)} \int_{1}^{\infty} \frac{d\lambda}{\sqrt{\lambda^{2n}-1}} = A. \quad (11)$$

Once again, the integral can be calculated:

$$\int_{1}^{\infty} \frac{d\lambda}{\sqrt{\lambda^{2n} - 1}} = \frac{-\sqrt{\pi}\Gamma(\frac{n-1}{2n})}{\Gamma(-\frac{1}{2n})},\tag{12}$$

yielding the acceleration during the K-AK interaction:

$$a = \left[\frac{-\sqrt{\pi}\Gamma(\frac{n-1}{2n})}{\Gamma(-\frac{1}{2n})} \right]^{2n/(n-1)} \frac{(n+1)(n+3)}{4} A^{2n/(1-n)}.$$
 (13)

An intriguing observation stems from the ratio of Eqs. (13) and (9). In particular, using the well-known identities $a\Gamma(a) = \Gamma(a+1)$, and $\Gamma(a)\Gamma(1-a) = \pi/1$ $\sin(\pi a)$, we can express the ratio of the K-AK to K-K forces as

$$R = \frac{F_{\text{K-AK}}}{F_{\text{K-K}}} = -\left[\sin\left(\frac{\pi}{2n}\right)\right]^{2n/(n-1)}.$$
 (14)

This expression suggests that, contrary to what is known about "standard" models such as sine-Gordon or φ^4 and their exponentially decaying kinks and antikinks [2,3,10], here the ratio of the K-AK to K-K force is *not* equal (in absolute value) to 1, but rather decreases with *n*. Therefore, a fundamental characteristic of long-range-interacting kinks is that this feature becomes more dramatic (with the ratio, in principle, tending to 0 as $n \to \infty$), as the tails become "heavier".

For n=2 (φ^8 model), from Eq. (13), we get $a=11.0785/A^4$ and $F=-\frac{2}{15}a=-1.4771/A^4$. Similarly, for n=3 (φ^{10} model), we get $a=2.0676/A^3$ and $F=-\frac{1}{12}a=-0.1723/A^3$. Finally, for n=4 (φ^{12} model), we get $a=1.2495/A^{8/3}$ and $F=-\frac{2}{35}a=-0.0714/A^{8/3}$. Armed with these specific predictions for K-K and K-AK interactions, we turn to verification of our general theory via direct numerical simulations.

Numerical results.—Here, we deploy our recent methodology [28], which is critical to obtaining accurate simulations of the interactions between topological defects with power-law tails (long-range interactions). Briefly, a pseudospectral differentiation matrix with periodic boundary conditions [30] replaces the spatial derivatives in Eq. (2) on the interval $x \in [-200, 200]$ with N = 2000 discrete points (hence, the grid spacing is $\Delta x = 0.2$). The resulting system of ordinary differential equation (ODE) (after discretizing in x) is integrated numerically using MATLAB's ODE45 solver with built-in error control.

Following Ref. [28], for the K-AK interactions we start with a "split-domain" ansatz $\varphi_{\rm split}(x) = [1-H(x)]\varphi_{(-1,0)}(x)+H(x)\varphi_{(0,-1)}(x)$, where H(x) is the Heaviside unit step function. That is, $\varphi_{\rm split}(x) = \varphi_{(-1,0)}(x)$ on the interval $(-\infty,0]$, while $\varphi_{\rm split}(x) = \varphi_{(0,-1)}(x)$ on the interval $(0,\infty)$. Then, $\varphi_{\rm split}(x)$ is used as the initializer for the MATLAB function LSQNONLIN, which minimizes (using nonlinear least squares) the l_2 norm of the discretized version of the opposite of the right-hand side of Eq. (2), subject to the two additional constraints of keeping the positions of the kink and antikink fixed. The result is a smoothed and minimized version of $\varphi_{\rm split}(x)$, which is then used as the initial condition for solving the partial differential equation (PDE) Eq. (2) numerically.

The K-K case is similar, except that $\varphi_{\rm split}(x) = [1-H(x)]\varphi_{(-1,0)}(x) + H(x)\varphi_{(0,1)}(x)$. As a result, there is a discontinuity at x=0, which becomes large for φ^{10} and even larger for φ^{12} . With N=2000, LSQNONLIN fails to converge for some cases; however, for smaller N it does converge. Thus, the output from smaller N can be used as the initializer for LSQNONLIN with N=2000, which then converges quickly. Except for this detail, the procedure is the same as for the K-AK case. As explained in Ref. [28], this type of minimization procedure is *crucial* in order to avoid inaccurate interaction observations stemming from a more naive sum or product (of kinks) ansatz.

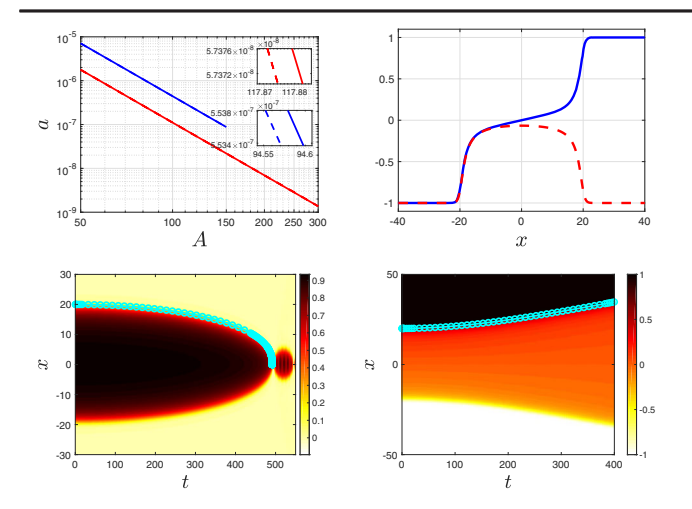


FIG. 1. Top left is the log-log plot of the left kink acceleration a as a function of A for the kink-kink interaction (blue) and kinkantikink interaction (red) in the φ^8 model. The dashed lines are computed numerically, and the solid lines are computed analytically. Top right is the plot of the initializers for the kink-kink (K-K) (blue-solid) and kink-antikink (K-AK) (red-dashed) interaction. Bottom left is the space-time contour plot of the K-AK interaction, and the cyan curve with circle symbols is the plot of the solution to the initial value problem (IVP): $\ddot{x}(t) =$ $-11.0785/x^4$, x(0) = 20, $\dot{x}(0) = 0$. Bottom right is the spacetime contour plot of the K-K interaction, and the cyan curve with circle symbols is the solution to the IVP: $\ddot{x}(t) = 44.3139/x^4$, $x(0) = 20, \dot{x}(0) = 0.$

F1:1

F1:2

F1:3

F1:4

F1:5

F1:6

F1:7

F1:8

F1:9

F1:10

F1:11

F1:12

F1:13

248

249

250

251

252

253

254

255

256

257

258

259

260

261

262

263 264

265

266

267

268

269

270

271

272

273

In Figs. 1–3, the top-right panel shows the K-K and K-AK configuration initializers used to evolve the PDE, i.e., Eq. (2), under the φ^8 , φ^{10} , and φ^{12} models, respectively. The bottom-left and bottom-right panels of each figure show, respectively, the space-time evolution of the field for the K-AK case (attraction) and K-K case (repulsion). Cyan curves with circle symbols are solutions to the Newtonian equation of motion Ma = F, where F was obtained above in the form $F = M\gamma_i(n)A^{2n/(1-n)}$ with $\gamma_i(n)$ as the corresponding prefactor (i = K-K or K-AK). Since $a = \ddot{A}$ for K-K and $a = -\ddot{A}$ for K-AK, then both cases require solving the initial value problem (IVP) for the kink location x = A: $\ddot{x} = \pm \gamma_i(n) x^{2n/(1-n)}$, $\dot{x}(0) = 0$, and x(0) given.

Note that in all three figures, especially in Figs. 2 and 3, the bottom-left plots show that the attractive force between the kink and antikink leads them to collide at x = 0 at some instant of time, upon which "bounces" are observed. Our theory of the interaction force is asymptotic for large separation; therefore it does not in any way address the instant of collision and beyond. Therefore, the cyan curves (with circle symbols) are not expected to agree with the contours of the numerical solution as the kink and antikink locations approach the origin (x = 0).

Next, we numerically calculate the relation between the location of the kink (i.e., half-separation) A and its

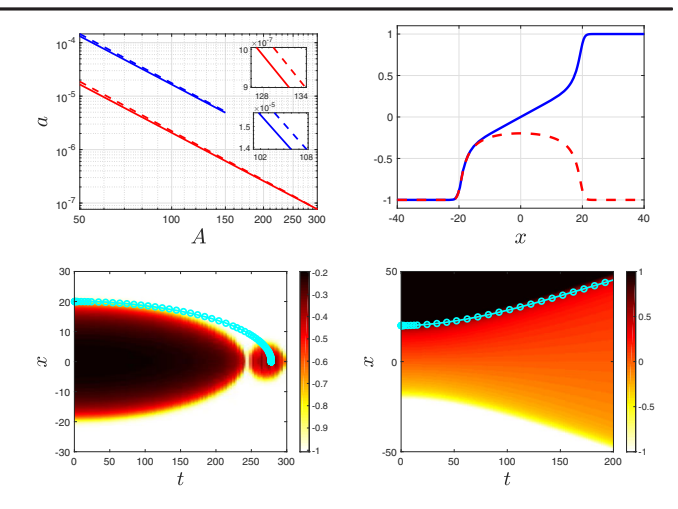


FIG. 2. Equivalent of Fig. 1 for the φ^{10} model. Bottom left is the space-time contour plot of the K-AK interaction, and the cyan curve with circle symbols is the solution to the IVP: $\ddot{x}(t) = -2.0676/x^3$, x(0) = 20, $\dot{x}(0) = 0$. Bottom right is the space-time contour plot of the K-K interaction, and the cyan curve with circle symbols is the solution to the IVP: $\ddot{x}(t) = 16.5411/x^3, x(0) = 20, \dot{x}(0) = 0.$

acceleration a (from rest) by solving the PDE in Eq. (2) over a very short time interval (from t = 0 to t = 0.01). A is then calculated as a function of t over this interval, which is used to estimate the acceleration $a = \ddot{A}$, which is nearly

constant during this time interval. Then, a least-squares model of the form $a = b/A^k$ was fit to the simulation data. The numerically fit results are shown graphically in log-log plots in the upper-left panels of Figs. 1–3. Therein, the numerically fit models are also compared to the results

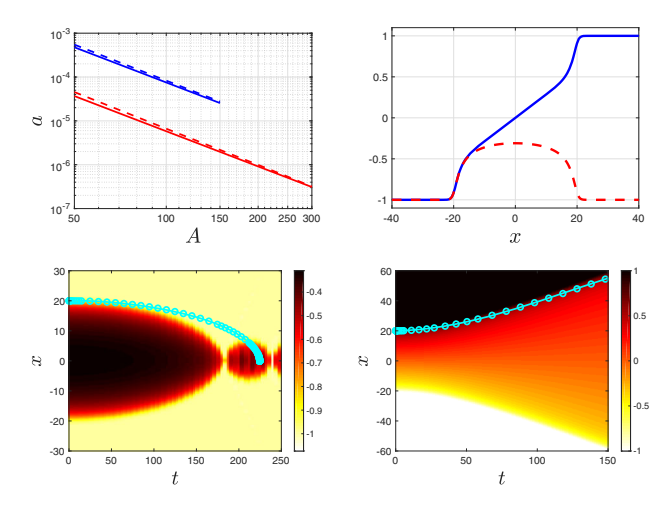


FIG. 3. Equivalent of Figs. 1 and 2 for the φ^{12} model. Bottom left is the space-time plot of the K-AK interaction, and the cyan curve with circle symbols is the solution to the IVP: $\ddot{x}(t) = -1.2495/x^{8/3}$, x(0) = 20, $\dot{x}(0) = 0$. Bottom right is the space-time contour plot of the K-K interaction, and the cyan curve with circle symbols is the solution to the IVP: $\ddot{x}(t) = 16.1871/x^{8/3}, \ \dot{x}(0) = 20, \ \dot{x}(0) = 0.$

F3:1

F3:2

F3:3

F3:4

F3:5

F3:6

F3:7

TABLE I. Theoretical model and numerical fit model predictions for the acceleration as a function of position during the kink-kink interaction. The error is the maximum relative error between the theory and fit curves over the specified range of A.

n	Theory	Fit	Range	Error
2	$44.31/A^4$	$43.43/A^{3.996}$	$50 \le A \le 150$	0.35%
3	$16.54/A^3$	$21.74/A^{3.046}$	$50 \le A \le 150$	10%
4	$16.19/A^{8/3}$	$23.23/A^{2.724}$	$50 \le A \le 150$	15%

from the theoretical analysis above. The fit between the asymptotic prediction and the numerical results is good in all the cases considered, and nearly perfect for the φ^8 model. The kink location predicted by solving the appropriate IVP is superimposed onto the contour plots in the bottom panels of Figs. 1–3.

In Tables I and II we summarize our findings, both theoretical and numerical. In calculating the error between the theoretical and numerical models we find that, for smaller values of A, the error between the models is greater (especially as n becomes larger). The reason for this discrepancy is twofold: (i) the theoretical model derived above is valid only asymptotically for large separations, and (ii) for large n, the domain walls exhibit "fatter" tails; thus it becomes increasingly difficult to prepare a "well-separated" initial condition. Therefore, we restrict ourselves to $A \geq 50$ when calculating the fit to the numerical simulation data and when comparing it against the theoretical prediction.

For the K-AK interaction, we used six A values (data points) in the interval [50, 300], while for the K-K interaction we used six A values in the interval [50, 150]. For the K-K case it is difficult to find accurate initial conditions for the PDE for A > 150 (because MATLAB's LSQNONLIN takes longer, or fails, to converge to an appropriate field configuration to be used as an initial condition). The relative error between the theoretical model and the numerical fit is calculated over the same range as the range of data points used to obtain the numerical models. In all cases, the maximum error occurs at the first data value (A = 50). A more computationally intensive investigation of the suitable distance regime in which the asymptotic theoretical predictions are valid may significantly reduce the error in Tables I and II for larger n. Thus,

TABLE II. Theoretical model and numerical fit model predictions for the acceleration as a function of position during the kinkantikink interaction. The error is the maximum relative error between the theory and fit curves over the specified range of A.

\overline{n}	Theory	Fit	Range	Erro
2	$11.08/A^4$	$10.92/A^{3.997}$	$50 \le A \le 300$	0.4%
3	$2.068/A^3$	$3/A^{3.064}$	$50 \le A \le 300$	13%
4	$1.25/A^{8/3}$	$2.234/A^{2.762}$	$50 \le A \le 300$	23%

on the basis of the currently available results, we conclude that further investigation would be required to determine such a range.

Conclusions and future work.—In the present work, we have taken a significant step beyond the standard fieldtheoretic models for topological defects and their interactions, which have been studied for a number of decades. Up to now, the vast majority of the associated onedimensional efforts have focused on kinks with exponential tail decay, thus endowing the coherent structures with a "short-range" exponential tail-tail interaction. Using potentials with the highest power going as ω^{2n+4} , for arbitrary n. as the vehicle of choice in this work, we have systematically examined the long-range pairwise kink-kink and kink-antikink interactions. We have blended state-of-theart asymptotic tools with carefully crafted numerical simulations to elucidate the power-law nature of the decay of the interaction force with the 2n/(n-1)th power of the separation between the topological defects. Equally important, we have identified the prefactor of this interaction (for arbitrary n) and have confirmed its agreement with numerical simulations for n = 2, n = 3, and n = 4.

Our results will likely provide valuable insights into domain wall interaction in materials [13,14] and biophysical [29] contexts that are governed by higher-order field theories. We also hope that this study will pave the way for the formulation of novel collective coordinate treatments [31] of long-range interactions, and a systematic understanding of their outcomes (including the role of initial kinetic energy; here, to crystallize the relevant phenomenology we restricted ourselves to kinks initially at rest). Another direction of future work concerns the exploration of coherent structures in higher dimensions [32] and the understanding of the existence, stability, and dynamics of localized and vortical patterns therein. Finally, the methodology developed herein can be applied to kink interactions in other recently proposed higher-order field theories harboring power-law tails [11,25,33].

This material is based upon work supported by the U.S. National Science Foundation under Grant No. PHY-1602994 and under Grant No. DMS-1809074 (P. G. K.). The work of MEPhI group was supported by the MEPhI Academic Excellence Project under Contract No. 02.a03.21.0005. V. A. G. also acknowledges the support of the Russian Foundation for Basic Research under Grant No. 19-02-00971. A. K. is grateful to INSA (Indian National Science Academy) for the award of INSA Senior Scientist position. A. S. was supported by the U.S. Department of Energy.

^[1] A. Vilenkin and E. P. S. Shellard, *Cosmic Strings and Other Topological Defects* (Cambridge University Press, Cambridge, England, 2000).

^[2] N. Manton and P. Sutcliffe, *Topological Solitons* (Cambridge University Press, Cambridge, England, 2004).

[3] R. K. Dodd, J. C. Eilbeck, J. D. Gibbon, and H. C. Morris,
 Solitons and Nonlinear Wave Equations (Academic Press,
 London, 1982).

376

377

378

379

380

381

382

383 384

385

386

387

388

389 390

391

392

393

394

395

396

397

398

399

400

401

402

403

404

405

406

407

408

409

410

411

412

413

- [4] L. D. Landau, On the theory of phase transitions (in Russian), Zh. Eksp. Teor. Fiz. 7, 19 (1937); V. L. Ginzburg and L. D. Landau, On the theory of superconductivity (in Russian), Zh. Eksp. Teor. Fiz. 20, 1064 (1950).
- [5] M. Tinkham, Introduction to Superconductivity (McGraw-Hill, New York, 1996).
- [6] A. R. Bishop, J. A. Krumhansl, and S. E. Trullinger, Solitons in condensed matter: A paradigm, Physica (Amsterdam) 1D, 1 (1980).
- [7] A. E. Kudryavtsev, Solitonlike solutions for a Higgs scalar field, Pis'ma v ZhETF 22, 178 (1975) [JETP Lett. 22, 82 (1975).]
- [8] D. K. Campbell, J. F. Schonfeld, and C. A. Wingate, Resonance structure in kink-antikink interactions in ϕ^4 theory, Physica (Amsterdam) **9D**, 1 (1983).
- [9] S. Dutta, D. A. Steer, and T. Vachaspati, Creating Kinks from Particles, Phys. Rev. Lett. 101, 121601 (2008).
- [10] P. G. Kevrekidis and J. Cuevas-Maraver, A Dynamical Perspective on the ϕ^4 Model: Past, *Present and Future* (Springer-Verlag, Heidelberg, 2019).
- [11] A. Khare, I. C. Christov, and A. Saxena, Successive phase transitions and kink solutions in ϕ^8 , ϕ^{10} , and ϕ^{12} field theories, Phys. Rev. E **90**, 023208 (2014).
- [12] Y. M. Gufan and E. S. Larin, Phenomenological consideration of isostructural phase transition, Dokl. Akad. Nauk SSSR **242**, 1311 (1978); [, Sov. Phys. Dokl. **23**, 754 (1978).]
- [13] B. Mroz, J. A. Tuszynski, H. Kiefte, and M. J. Coulter, On the ferroelastic phase transition of LiNH₄SO₄: A Brillouin scattering study and theoretical modelling, J. Phys. Condens. Matter 1, 783 (1989).
- [14] S. V. Pavlov and M. L. Akimov, Phenomenological theory of isomorphous phase transitions, Crystallogr. Rep. (Transl. Kristallografiya) 44, 297 (1999).
- [15] F. J. Buijnsters, A. Fasolino, and M. I. Katsnelson, Motion of Domain Walls and the Dynamics of Kinks in the Magnetic Peierls Potential, Phys. Rev. Lett. 113, 217202 (2014).
- 414 [16] D. Bazeia and F. S. Bemfica, From supersymmetric quantum mechanics to scalar field theories, Phys. Rev. D **95**, 085008 (2017).
- 417 [17] A. Demirkaya, R. Decker, P. G. Kevrekidis, I. C. Christov, 418 and A. Saxena, Kink dynamics in a parametric ϕ^6 system: A 419 model with controllably many internal modes, J. High 420 Energy Phys. 12 (2017) 071.
- 421 [18] P. Dorey, K. Mersh, T. Romanczukiewicz, and Y. Shnir,
 422 Kink-Antikink Collisions in the φ⁶ Model, Phys. Rev. Lett.
 423 107, 091602 (2011); V. A. Gani, A. E. Kudryavtsev, and

- M. A. Lizunova, Kink interactions in the (1+1)-dimensional φ^6 model, Phys. Rev. D **89**, 125009 (2014); A. Moradi Marjaneh, V. A. Gani, D. Saadatmand, S. V. Dmitriev, and K. Javidan, Multi-kink collisions in the ϕ^6 model, J. High Energy Phys. 07 (2017) 028.
- [19] M. A. Amin, E. A. Lim, and I.-S. Yang, Clash of Kinks: Phase Shifts in Colliding Nonintegrable Solitons, Phys. Rev. Lett. 111, 224101 (2013); A scattering theory of ultrarelativistic solitons, Phys. Rev. D 88, 105024 (2013).
- [20] M. A. Lohe, Soliton structures in $P(\varphi)_2$, Phys. Rev. D **20**, 3120 (1979).
- [21] B. A. Mello, J. A. González, L. E. Guerrero, and E. López-Atencio, Topological defects with long-range interactions, Phys. Lett. A 244, 277 (1998).
- [22] D. Bazeia, M. A. González León, L. Losano, and J. Mateos Guilarte, Deformed defects for scalar fields with polynomial interactions, Phys. Rev. D 73, 105008 (2006); New scalar field models and their defect solutions, Europhys. Lett. 93, 41001 (2011).
- [23] A. R. Gomes, R. Menezes, and J. C. R. E. Oliveira, Highly interactive kink solutions, Phys. Rev. D 86, 025008 (2012).
- [24] V. A. Gani, V. Lensky, and M. A. Lizunova, Kink excitation spectra in the (1+1)-dimensional φ^8 model, J. High Energy Phys. 08 (2015) 147.
- [25] D. Bazeia, R. Menezes, and D. C. Moreira, Analytical study of kinklike structures with polynomial tails, J. Phys. Commun. 2, 055019 (2018).
- [26] E. Belendryasova and V. A. Gani, Scattering of the φ^8 kinks with power-law asymptotics, Commun. Nonlinear Sci. Numer. Simul. **67**, 414 (2019).
- [27] N. S. Manton, Forces between kinks and antikinks with long-range tails, J. Phys. A 52, 065401 (2019); arXiv: 1810.00788.
- [28] I. C. Christov, R. J. Decker, A. Demirkaya, V. A. Gani, P. G. Kevrekidis, and R. V. Radomskiy, Long-range interactions of kinks, Phys. Rev. D 99, 016010 (2019).
- [29] A. A. Boulbitch, Crystallization of proteins accompanied by formation of a cylindrical surface, Phys. Rev. E 56, 3395 (1997).
- [30] L. N. Trefethen, Spectral Methods in Matlab (Society for Industrial and Applied Mathematics, Philadelphia, PA, 2000)
- [31] I. Takyi and H. Weigel, Collective Coordinates in onedimensional soliton models revisited, Phys. Rev. D 94, 085008 (2016).
- [32] P. Ahlqvist, K. Eckerle, and B. Greene, Kink collisions in curved field space, J. High Energy Phys. 04 (2015) 59.
- [33] A. Khare and A. Saxena, Family of potentials with power-law kink tails, arXiv:1810:12907.

472 473 474

424

425

426

427

428

429

430

431

432

433

434

435

436

437

438

439

440

441

442

443

444

445

446

447

448

449

450

451

452

453

454

455

456

457

458

459

460

461

462

463

464

465

466

467

468

469

470

471